В совокупности рассмотренные аспекты показывают, что образование слоя льда на поверхности Au (111) является многофакторным процессом, зависящим не только от природы адсорбата и подложки, но и от кинетики, структуры поверхности и внешних условий. Такое комплексное понимание процессов адсорбции и самоорганизации воды расширяет возможности контроля молекулярных систем на наноуровне и способствует развитию современной физики поверхности.

Заключение. Образование слоя льда на поверхности Au (111) представляет собой сложный физико-химический процесс, определяемый взаимодействием молекул воды между собой и с металлической подложкой. Несмотря на химическую инертность золота, молекулы воды способны формировать устойчивые и упорядоченные двумерные структуры за счет развития сети водородных связей. Экспериментальные исследования показывают, что геометрия и стабильность ледяных слоев зависят от температуры, степени покрытия и особенностей реконструкции поверхности Au (111). А также изучены десорбции молекул воды при малоэнергетической ионной бомбардировке и показаны механизмы десорбции их от поверхности. Полученные результаты имеют важное значение для фундаментального понимания процессов адсорбции и фазовых переходов в низкоразмерных системах, а также могут быть использованы при разработке функциональных поверхностей и наноструктурированных материалов.

Список использованной литературы:

(1). Verdaguer A., Sacha G.M., Bluhm H., Salmeron M. Molecular structure of water at interfaces: Wetting at the nanometer scale. Chemical Reviews. 2016, vol. 106, № 4, p. 1478–1510.

(2). Michaelides A., Morgenstern K. Ice nanoclusters at hydrophobic metal surfaces. Nature Materials, 2017, vol. 6, p. 597–601.

(3). Morgenstern K., Michely T., Comsa G. Scanning tunneling microscopy studies of ice formation on metal surfaces. Surface Science. 2012, vol. 497, p. 1–13.

(4). Thürmer K., Bartelt N.C. Growth dynamics of ice on Pt (111). A molecular view. Physical Review B. 2018, vol. 77, 195425.

(5). W.Ekstein. “Computer simulation of ion-solid collision”. Springer-Verlag, p. 341–348, 1991.

(6). Евдокимов И.Н. “Взаимосвязь эффектов рассеяния и распыления при ионной бомбардировке поверхности кристаллов”, Поверхность, №8. с. 31–38, 1988.

(7). Курнаев В.А., Машкова Е.С., Молчанов В.М. “Отражения легких ионов от поверхности твердого тела”, Москва, 1985, с. 192.

(8). “Sputtering by Particle Bombardment II”. Ed.by R. Behrisch. Berlin–Heidelberg–New York–Tokyo: Springer–Verlag, 1983.

(9).Frenkel D., Smit B. “Understanding molecular simulation”. Academic Press. Amsterdam, 2001, ISBN 0-12-267351-4.

(10). Schlick T. “Molecular modeling and simulation”. Springer. Amsterdam, 2002. ISBN 0-387-95404-X.

Kurbanov Davron Shavkatovich (Urgench State University named after Abu Rayhon Beruni, senior lecturer; davronkurbanow89@gmail.com),
Yakubov Komlijon Ruzmetovich (Urgench State University named after Abu Rayhon Beruni, associate professor),
Bazarbayev Rustam Bahrambayevich (Urgench State University named after Abu Rayhon Beruni, PhD, associate professor),
Rakhimboyev Rakhmatjon Shavkat oglu (PhD student, Urgench State University named after Abu Rayhon Beruni)

IMPACT OF Fe DOPING ON THE ELECTRONIC STRUCTURE OF KAOLINITE

Annotation. *Hybrid functional density functional theory calculations were employed to investigate the effect of iron (Fe) doping on the electronic properties of kaolinite ($Al_2Si_2O_9H_4$). The results show that pristine kaolinite has a wide band gap of 6.24 eV, which significantly decreases to 2.8 eV when Fe is introduced at a concentration of 25% relative to silicon atoms (2.94% of total atoms). Density of states analysis reveals that Fe d-orbitals are primarily responsible for the band gap reduction. Bader charge and electron localization analyses indicate a decrease in electron density around oxygen atoms bonded to iron. As a result, Fe doping induces semiconducting behavior and enhances photosensitivity, suggesting potential applications in solar energy conversion, photocatalysis, and sensor technologies.*

Key words: *Kaolin, DFT, VASP, PBE, GGA, PAW, HSE06*

KAOLIN ELEKTRON TUZILISHIGA Fe KIRITMASINING TA’SIRI

Annotatsiya*. Ushbu ishda gibrid funksional zichlik funksional nazariyasi asosida temir (Fe) dopingi kaolinit ($Al_2Si_2O_9H_4$)ning elektron xususiyatlariga ta’siri o‘rganildi. Sof kaolinitning tarmoqli oralig‘i 6.24 eV bo‘lib, Fe dopingi 25% (Si atomlariga nisbatan) kiritilganda u 2.8 eVgacha kamayadi. Holatlar zichligi tahlili tarmoqli oralig‘ining qisqarishida Fe ning d-orbitallari asosiy rol o‘ynashini ko‘rsatdi. Bader zar-*

yad va elektron lokalizatsiya tahlillari temir bilan bog'langan kislorod atomlari atrofida elektron zichligining kamayganligini tasdiqlaydi. Natijada, Fe bilan doplangan kaolinit yarimo'tkazgich xususiyatlariga ega bo'lib, fotosensitivligi ortadi va uni quyosh energetikasi, fotokataliz hamda sensor texnologiyalarida qo'llash imkonini beradi.

Kalit so'zlar: *Kaolin, DFT, VASP, PBE, GGA, PAW, HSE06.*

ВЛИЯНИЕ ЛЕГИРОВАНИЯ FE НА ЭЛЕКТРОННУЮ СТРУКТУРУ КАОЛИНА

Аннотация. *В работе с использованием гибридных функционалов теории функционала плотности исследовано влияние легирования железом (Fe) на электронные свойства каолинита ($Al_2Si_2O_9H_4$). Установлено, что ширина запрещённой зоны чистого каолинита составляет 6.24 эВ и уменьшается до 2.8 эВ при введении Fe в концентрации 25% по отношению к атомам кремния. Анализ плотности состояний показал, что уменьшение запрещённой зоны обусловлено d-орбиталями Fe. Результаты анализа зарядов по Бадеру и локализации электронов указывают на снижение электронной плотности вокруг атомов кислорода, связанных с железом. В результате легирования материал приобретает полупроводниковые свойства и повышенную фоточувствительность, что делает его перспективным для применения в солнечной энергетике, фотокатализе и сенсорных технологиях*

Ключевые слова*: Каолин, DFT, VASP, PBE, GGA, PAW, HSE06.*

Introduction. In modern materials physics and chemistry, clay minerals, particularly kaolin ($Al_2Si_2O_9H_4$), are widely used due to their unique structural and chemical properties. Kaolin is a natural white clay, and its crystal structure consists of aluminosilicate layers [1]. Modifying the electronic properties of this material, particularly by reducing its band gap value, has expanded its application possibilities in important technological areas such as semiconductors, photocatalysis, and sensors [2].

Doping with transition metal ions is considered an effective method for changing the electronic, optical and magnetic properties of materials. Among these, Iron (Fe) is of particular interest. More specifically, it can exist in various oxidation states and significantly changes its electronic properties when introduced into the kaolin structure [3]. Fe-doped kaolin is considered a promising material for many practical applications such as reducing environmental pollution, catalysts and light absorption systems [4].

Modern computational methods, especially density functional theory (DFT), allow the study of fundamental properties of clay minerals at the atomistic level [5]. Hybrid functionals, particularly HSE06, are of special importance for accurately calculating the band gap values of materials. Standard DFT methods often underestimate band gap values [6].

In this research, we studied the changes in the electronic properties of kaolin by doping it with iron atoms. Our main focus was on the changes in electronic localization, Bader charge distribution, and band gap values of Fe-doped kaolin. Understanding these changes opens up possibilities for expanding the practical applications of kaolin-based materials and creating materials with new functional properties [7].

Using DFT calculations performed with the Vienna Ab-initio Simulation Package (VASP), the crystal structure, electronic properties of kaolin, and changes resulting from Fe doping were analyzed in detail. The research results have wide-ranging practical significance, expanding the possibilities of using kaolin-based materials in areas such as photocatalysis, gas sensors, and solar energy utilization [8,9,10].

Computational Methodology. The computations were executed with the Vienna Ab-initio Simulation Package (VASP6.5), with structural optimization conducted via the Projector Augmented Wave (PAW) method, parameterized by Perdew, Burke, and Ernzerhof (PBE), employing the generalized gradient approximation (GGA). The DFT-D3 method was incorporated to account for Van der Waals interactions during structure optimization. For band gap calculations, the Heyd-Scuseria-Ernzerhof 2006 (HSE06) hybrid functional was used. The cutoff energy was 620 eV. For system geometry optimization, force convergence of 0.02 eV/Å and energy convergence of 10^{-5} eV were used. For Brillouin zone sampling, gamma-centered k-point grids of 4 × 3 × 2 were used [11,12,13,14,15]. Calculations were performed using the above criteria for both before and after Fe doping of kaolinite.

Results and discussion. The structure of kaolinite ($Al_2Si_2O_9H_4$) was optimized according to established criteria. Structural optimization utilizing the Perdew-Burke-Ernzerhof (PBE) func-tional yielded lattice parameters and angular values of a=5.1756 Å, b=7.3398 Å, c=8.98 Å, α=91.70°, β=89.80°, and γ=105.10°, which demonstrated excellent agreement with experimental results [2]. Subsequent optimization following iron incorporation as an impurity resulted in modified lattice parameters and angular values of a=5.17886 Å, b=7.361 Å, c=9.027 Å, α=91.44°, β=90.25°, and γ=105.18° (Fig.1). These structural modifications induced significant alterations in charge transfer mechanisms, electron localization patterns, and electronic band structure of the material.

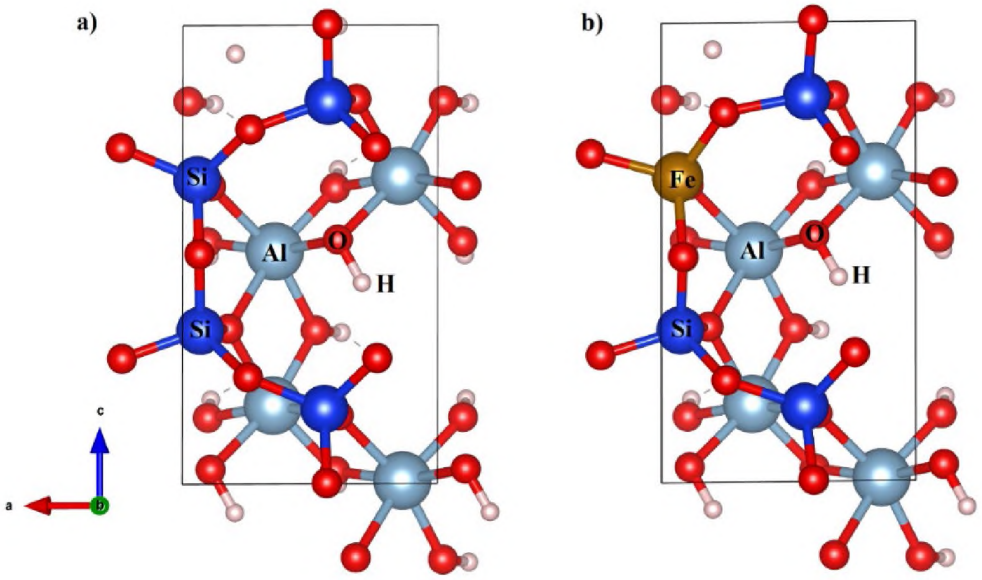


Fig 1. Optimized structures of kaolinite before (a) and after (b) Fe doping.

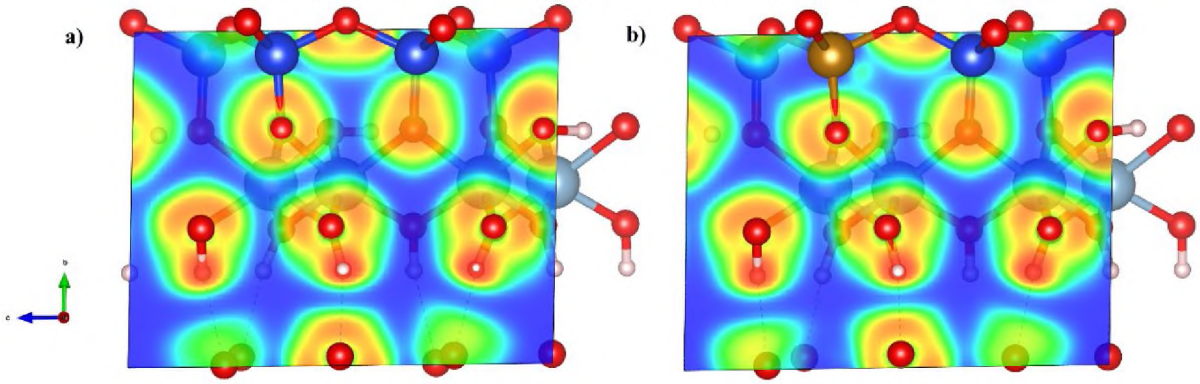


Fig 2. Electron localization distribution in kaolinite before (a) and after (b) Fe doping.

Electron localization, Bader charge analysis, and band structure were calculated using the HSE06 hybrid functional for the state before and after iron doping. When examining the electron localization and Bader charge analysis, we observe that after iron doping, the electron acceptance of oxygen atoms that formed bonds with iron was reduced. This phenomenon is attributable to iron's larger ionic radius compared to silicon and its diminished electron-donating capacity. The validity of these hypotheses is further corroborated by Bader charge calculations, which revealed that in the pristine structure (case a), the charge distribution was Si(+3.22e)–O(-1.62e), whereas in the Fe-doped structure (case b), the distribution shifted to Fe(+1.67e)–O(-1.11e) (Fig. 2, 3). These findings indicate that iron transfers fewer electrons to oxygen compared to silicon. The incomplete participation of iron's valence electrons in bonding resulted in reduced electron localization around the oxygen atoms (Fig. 2, 3).

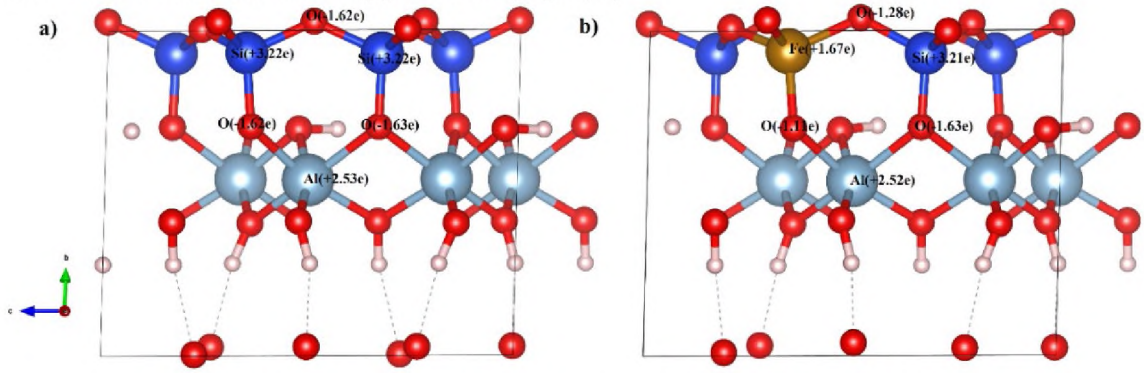


Fig 3. Bader charge analysis of kaolinite before (a) and after (b) Fe doping.

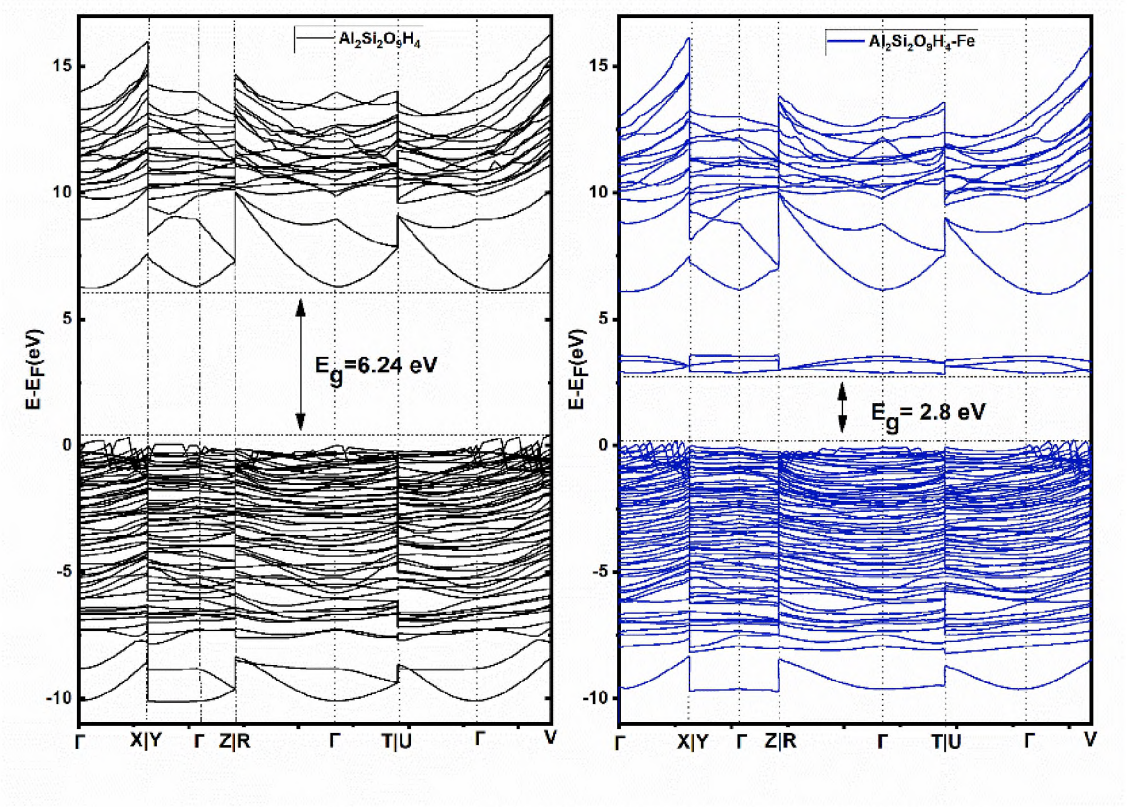


Fig 4. Band structure of kaolinite before (a) and after (b) Fe doping.

Before Fe doping, the calculated band gap of kaolin was 6.24 eV [2]. After iron doping, the band gap value dropped sharply. The resulting band gap value became equal to 2.8 eV. The large number of valence electrons in iron causes the appearance of additional electron levels in the lower part of the conduction band. As a result, electrons with less energy quickly transfer from the valence band to the conduction band. After the introduction of iron, the distance between kaolin atoms increased significantly. As a result, the lattice constant also increased. This additionally contributed to the decrease in the band gap[16,17].

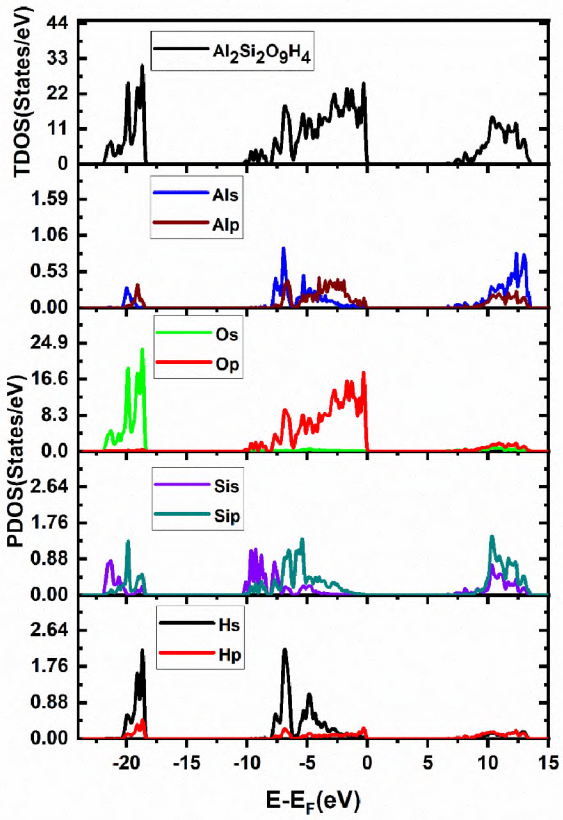


Fig 5. Density of full and partial electronic states before adding Fe to kaolin.

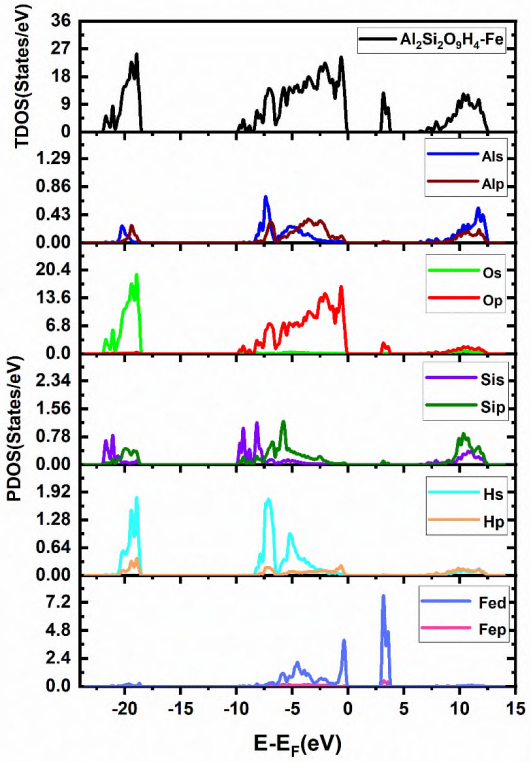


Fig 6. Density of full and partial electronic states after the introduction of Fe into kaolin.

When we look at the density of complete and partial electron states in the state before the introduction of iron into kaolin, we see that the electron states in the conduction band are mainly created by the s orbitals of aluminum and silicon and the p orbitals of oxygen. In the upper part of the valence band, we see that the number of electron states in the p orbital of oxygen has increased. This indicates that oxygen has accepted electrons. When iron is introduced, an additional electron state appears in the forbidden band. This electron state is created by the d orbital of iron and the p orbital of oxygen (Fig. 5, 6).

Conclusion. Electron localization, bader charge, band gap change and density of electronic states were determined for the states before and after Fe doping of kaolin. In particular, the electron acceptance of oxygen that formed bonds with iron decreased. Electron localization analysis revealed that the electron cloud has shrunk. The results obtained in the Bader charge analysis also confirmed this. Before iron was introduced, the electron acceptance of oxygen was equal to O(-1.62e), after iron was introduced, it became O(-1.11e). The band gap was 6.28 eV before iron was introduced, and became equal to 2.8 eV after iron was introduced. The fact that the band gap is 2.8 eV indicates that it can be used as a semiconductor. The reduction of the band gap was found to be caused by the d orbital of Fe by determining the density of electronic states. These important fundamental results obtained in atomistic calculations serve as an important foundation for increasing the possibility of application in modern electronic devices, highly sensitive gas sensors, semiconductors, photocatalysis and solar energy utilization.

References:

(1). Murray HH. Applied clay mineralogy: occurrences, processing and applications of kaolins, bentonites, palygorskite-sepiolite, and common clays. Elsevier, 2006.

(2). Nisar J., Topalian Z., De Sarkar A., Österlund L., Ahuja R. Optical gap and native point defects in kaolinite studied by the GGA-PBE, HSE functional, and GW approaches. Physical Review B. 2011;84(7):075135.

(3). Fu L., Yang H. Structure and electronic properties of transition metal doped kaolinite nanoclay. Nanoscale Research Letters. 2017, 12(1), p. 411.

(4). Chen M., Yang T., Han J, et al. The Application of Mineral Kaolinite for Environment Decontamination: A Review. Catalysts. 2023, 13(1), p. 123.

(5). Richard N., Zalutskii AA. et al. Local Environments in Iron-Bearing Clay Minerals by DFT Approaches. Applied Clay Science. 2021;214:106277.

(6). Apaolaza-Goikoetxea A., Richard N., Rendtorff NM., Gil Rebaza AV. The study of their structural and electronic properties by DFT methods. Applied Clay Science. 2022, 218, 106404.

(7). Zhao J., Qin X., Wang J., He M. Effect of Mg (II) and Na(I) doping on the electronic structure and mechanical properties of kaolinite. Minerals. 2020, 10(4), p. 368.

(8). Fakhri M.A., Abdallah B. et al. Enhancing photocatalytic performance of kaolin clay: an overview of treatment strategies and applications. Journal of Materials Science. 2023, 58, pp. 18123-18147.

(9). Cuong N.D., Hoa N.D. et al. Thermally reduced kaolin-graphene oxide nanocomposites for gas sensing application. Scientific Reports. 2015, 5, p. 7676.

(10). Chen Y., Wen L., Chen J., Luo H., Liu J. In situ growth of g-C3N4 on clay minerals of kaolinite, sepiolite, and talc for enhanced solar photocatalytic energy conversion. Applied Clay Science. 2022, 216, p. 106337.

(11). Blöchl P.E. Projector augmented-wave method. Physical Review B. 1994;50(24):17953-17979.

(12). Perdew J.P., Burke K., Ernzerhof M. Generalized gradient approximation made simple. Physical Review Letters. 1996, 77(18), p. 3865–3868.

(13). Grimme S., Antony J., Ehrlich S., Krieg H. A consistent and accurate ab initio parametrization of density functional dispersion correction (DFT-D) for the 94 elements H-Pu. The Journal of Chemical Physics. 2010, 132 (15), p. 154104.

(14). Heyd J., Scuseria G.E., Ernzerhof M. Hybrid functionals based on a screened Coulomb potential. The Journal of Chemical Physics. 2003, 118(18), pp. 8207–8215.

(15). Kresse G., Furthmüller J. Efficient iterative schemes for ab initio total-energy calculations using a plane-wave basis set. Physical Review B. 1996, 54(16), pp. 11169–11186.

(16). David L. Bish. Rietveld Refinement of the Kaolinite Structure at 1.5 K. Clays and Clay Minerals, Volume 41, Issue, December 1993, pp. 738 – 744. DOI: https://doi.org/10.1346/CCMN.1993.0410613

(17). Eman A., Alghamdi, Refka Sai. Impact of alloying iron pyrite by ruthenium on its band gap values and its insight to photovoltaic performance. Heliyon. 2023 Sep 19;9(10):e20270. doi: 10.1016/j.heliyon.2023.e20270

Sharipova Shohista Bakbergan qizi (Teacher at Urgench State University named after Abu Rayhan Beruni), Bozorboyeva Shoira Shavkatovna (Student at Urgench State University named after Abu Rayhan Beruni; e-mail: shshb1990@gmail.com)

UNSTATIONARY FLOW OF MAXWELLIAN FLUID IN A CYLINDRICAL PIPE: ANALYTICAL SOLUTION

Annotation. *This study addresses the analytical problem of the unsteady flow of a rheologically complex fluid, specifically a Maxwellian fluid, within a cylindrical pipe under the influence of a constant pressure gradient. While stationary and oscillatory flows have been extensively studied, the transition processes in unsteady flows–where the fluid shifts from rest to a specific motion state–require deeper analytical exploration. This research aims to fill the scientific gap in theoretical models for non-stationary processes, which is vital for applications in biomedical engineering and hydraulic reliability.*

Keywords: *Maxwell's fluid, unsteady flow, cylindrical pipe, Laplace–Carson transform, Bessel functions, relaxation time, Poiseuille flow.*

SILINDRSIMON QUVURDA MAKSVEL SUYUQLIGINING NOSTATSIONAR OQIMI: ANALITIK YECHIM

Annotatsiya*. Ushbu tadqiqot reologik jihatdan murakkab suyuqlik, xususan, Maxwell fluidning doimiy bosim gradienti ta'sirida silindrsimon quvur ichidagi nostatsionar oqimining analitik masalasini ko'rib chiqadi. Statsionar va tebranishli oqimlar yetarlicha o'rganilgan bo'lsa-da, nostatsionar oqimlarda, ya'ni suyuqlikning tinch holatdan ma'lum harakat holatiga o'tish jarayonlari chuqurroq analitik tahlilni talab etadi. Mazkur tadqiqot nostatsionar jarayonlar uchun nazariy modellar sohasidagi ilmiy bo'shliqni to'ldirishga qaratilgan bo'lib, bu yo'nalish biotibbiyot muhandisligi hamda gidravlik tizimlar ishonchliligi uchun muhim ahamiyat kasb etadi.*

Kalit so'zlar*: Maksvel suyuqligi, nostatsionar oqim, silindrsimon quvur, Laplace–Carson transform, Bessel functions, relaksatsiya vaqti, Poiseuille flow.*

НЕСТАЦИОНАРНОЕ ТЕЧЕНИЕ МАКСВЕЛЛОВСКОЙ ЖИДКОСТИ В ЦИЛИНДРИЧЕСКОЙ ТРУБЕ: АНАЛИТИЧЕСКОЕ РЕШЕНИЕ

Аннотация*. В данной работе рассматривается аналитическая задача нестационарного течения реологически сложной жидкости, в частности, Maxwell fluid – в цилиндрической трубе под действием постоянного градиента давления. Несмотря на то, что стационарные и колебательные течения были подробно исследованы, переходные процессы в нестационарных режимах, когда жидкость переходит из состояния покоя к определённому режиму движения, требуют более глубокого аналитического анализа. Настоящее исследование направлено на восполнение научного пробела в области теоретических моделей нестационарных процессов, что имеет важное значение для биомедицинской инженерии и обеспечения надёжности гидравлических систем.*

Ключевые слова*: максвелловская жидкость, нестационарное течение, цилиндрическая труба, Laplace–Carson transform, Bessel functions, время релаксации, Poiseuille flow.*

Introduction. The study of unsteady fluid flows is a fundamental aspect of modern fluid mechanics,